Article

Self-Assembly of Multidomain Peptides: Balancing Molecular Frustration Controls Conformation and Nanostructure

He Dong, Sergey E. Paramonov, Lorenzo Aulisa, Erica L. Bakota, and Jeffrey D. Hartgerink

J. Am. Chem. Soc., **2007**, 129 (41), 12468-12472• DOI: 10.1021/ja072536r • Publication Date (Web): 26 September 2007

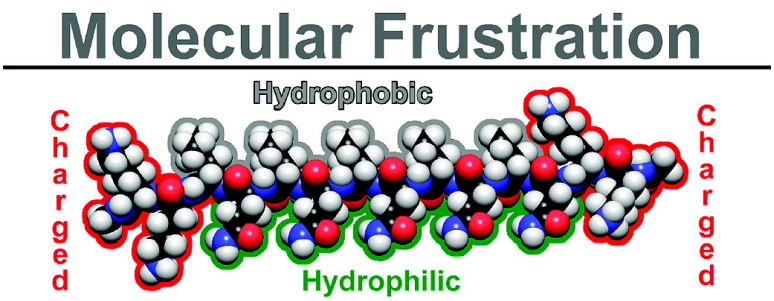

More About This Article

Additional resources and features associated with this article are available within the HTML version:

- Supporting Information
- Links to the 10 articles that cite this article, as of the time of this article download
- Access to high resolution figures
- Links to articles and content related to this article
- Copyright permission to reproduce figures and/or text from this article

View the Full Text HTML

J|A|C|S
ARTICLES
Published on Web 09/26/2007

Self-Assembly of Multidomain Peptides: Balancing Molecular Frustration Controls Conformation and Nanostructure

He Dong, Sergey E. Paramonov, Lorenzo Aulisa, Erica L. Bakota, and Jeffrey D. Hartgerink*

Contribution from the Departments of Chemistry and Bioengineering, Rice University, 6100 Main Street, Houston, Texas 77005

Received April 23, 2007; Revised Manuscript Received August 6, 2007; E-mail: jdh@rice.edu

Abstract: A series of nine, frustrated, multidomain peptides is described in which forces favoring self-assembly into a nanofiber versus those favoring disassembly could be easily modified. The peptides are organized into an **ABA** block motif in which the central **B** block is composed of alternating hydrophilic and hydrophobic amino acids (glutamine and leucine, respectively). This alternation allows the amino acid side chains to segregate on opposite sides of the peptide backbone when it is in a fully extended β-sheet conformation. In water, packing between two such peptides stabilizes the extended conformation by satisfying the desire of the leucine side chains to exclude themselves from the aqueous environment. Once in this conformation intermolecular backbone hydrogen bonding can readily take place between additional peptides eventually growing into high aspect ratio fibers. **B** block assembly may continue infinitely or until monomeric peptides are depleted from solution which results in an insoluble precipitate. Block **A** consists of a variable number of positively charged lysine residues whose electrostatic repulsion at pH 7 works against the desire of the **B** block to assemble. Here we show that balancing the forces of block **A** against **B** allows the formation of controlled length, individually dispersed, and fully soluble nanofibers with a width of 6 ± 1 nm and length of 120 ± 30 nm. Analysis by infrared, circular dichroism, and vitreous ice cryo-transmission electron microscopy reveals that the relative sizes of blocks **A** and **B** dictate the peptide secondary structure which in turn controls the resulting nanostructure. The system described epitomizes the use of molecular frustration in the design of finite self-assembled structures. These materials, and ones based on their architecture, may find applications where nanostructured control over fiber architecture and chemical functionality is required.

Introduction

Self-assembly is one of the most powerful ways to prepare nanostructured materials. Proper design of small, easy to synthesize, assemblers can lead to the organization of two or many thousands of these units into complex materials. Self-assembling structures can be categorized in many ways. One way is to divide them into "infinitely" assembling systems in which one or more of the dimensions' assembly is uncontrolled and finitely assembling systems in which all dimensions of assembly are controlled. Infinite assemblers include crystal engineering (3-dimensional),[1] self-assembled monolayers (2-dimensional),[2] cylindrical micelles,[3] and self-assembling nanofibers (1-dimensional)[4−7] among many others.[8−10] Finitely assembling systems can be prepared by design of specific interactions which limit the system's size. Examples of such systems include the DNA *double* helix, collagen *triple* helix, and coiled-coil *four* helix bundle. Another approach to finite assemblers is through the utilization of "molecular frustration" in which two or more components of the assembler have opposing preferences for solvation environment, attraction versus repulsion, and/or compact and ordered packing versus disordered packing.[11−14] In this paper we describe a multidomain peptide (MDP) which utilizes molecular frustration to control the organization and extent of assembly. When forces favoring assembly are properly balanced with forces favoring disassembly discrete nanofibers with controlled length result. This architectural motif may be utilized for novel tissue regeneration

(1) Braga, D.; Grepioni, F.; Desiraju, G. R. *Chem. Rev.* **1998**, *98*, 1375−1405.
(2) Yan, L.; Huck, W. T. S.; Whitesides, G. M. *Supramolecular Polymers*, 2nd ed; Ciferri, A., Ed.; CRC Press: Boca Raton, FL, 2005; pp 617−649.
(3) Won, Y.-Y.; Davis, H. T.; Bates, F. S. *Science* **1999**, *283*, 960−963.
(4) Hartgerink, J. D.; Beniash, E.; Stupp, S. I. *Science* **2001**, *294*, 1684−1688.
(5) Lamm, M. S.; Rajagopal, K.; Schneider, J. P.; Pochan, D. J. *J. Am. Chem. Soc.* **2005**, *127*, 16692−16700.
(6) Paramonov, S. E.; Jun, H.-W.; Hartgerink, J. D. *J. Am. Chem. Soc.* **2006**, *128*, 7291−7298.
(7) Pandya, M. J.; Spooner, G. M.; Sunde, M.; Thorpe, J. R.; Rodger, A.; Woolfson, D. N. *Biochem.* **2000**, *39*, 8728−8734.
(8) Pagel, K.; Wagner, S.; Samedov, K.; von Beriepsch, H.; Bottcher, C.; Koksch, B. *J. Am. Chem. Soc.* **2006**, *128*, 2196−2197.
(9) Vauthey, S.; Santoso, S.; Gong, H. Y.; Watson, N.; Zhang, S. G. *Proc. Natl. Acad. Sci.* **2002**, *99*, 5355−5360.
(10) von Maltzahn, G.; Vauthey, S.; Santoso, S.; Zhang, S. G. *Langmuir* **2003**, *19*, 4332−4337.
(11) Zubarev, E. R.; Pralle, M. U.; Li, L.; Stupp, S. I. *Science* **1999**, *283*, 523−526.
(12) Zubarev, E. R.; Pralle, M. U.; Sone, E. D.; Stupp, S. I. *J. Am. Chem. Soc.* **2001**, *123*, 4105−4106.
(13) Klok, H.-A.; Hwang, J. J.; Hartgerink, J. D.; Stupp, S. I. *Macromol.* **2002**, *35*, 6101−6111.
(14) Li, Z.; Kesselman, E.; Talmon, Y.; Hillmyer, M. A.; Lodge T. P. *Science* **2004**, *306*, 98−101.

10.1021/ja072536r CCC: $37.00

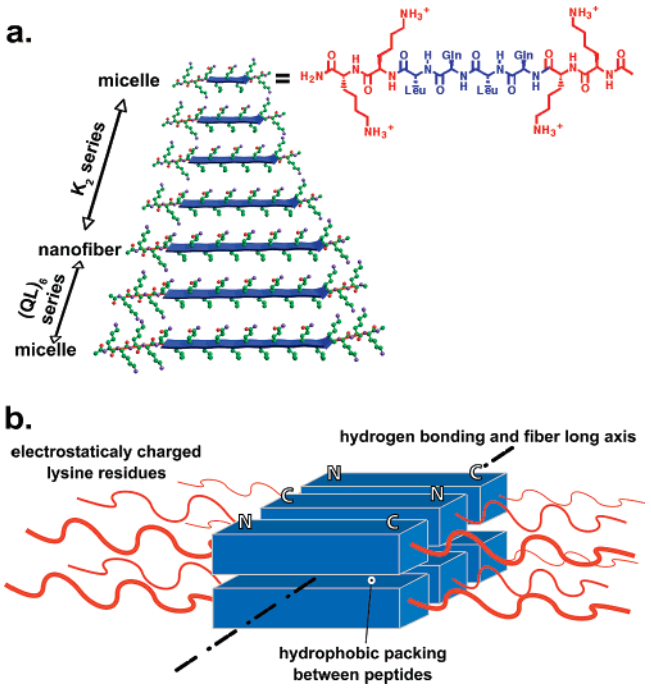

Figure 1. (a) Primary structures of the K_2 and $(QL)_6$ series of peptides showing the comparative domain size. (b) Proposed model of nanofiber self-assembly indicating hydrophobic packing region, axis of hydrogen bonding, and repulsive positive charges.

strategies and other systems which require control over chemical organization at the nanoscale.

Results and Discussion

MDPs (Figure 1) were designed with an **ABA** block motif. The central **B** block consists of a variable number of glutamine−leucine(QL) repeats. The alternating hydrophilic−hydrophobic pattern allows all glutamine side chains to lie on one face of the peptide and leucine side chains on the other when in an extended conformation creating a facial amphiphile. In aqueous environment there will be a significant driving force for two of these hydrophobic faces to pack against one another forming a hydrophobic sandwich which consequently stabilizes the fully extended conformation.[5,8−10,15−23] An intermolecular β-sheet hydrogen-bonding network can then be created between two or more pairs of these sandwiches. The extension of the hydrogen-bonding network into long fibers is reminiscent of natural and synthetic mimics of amyloid nanofibers.[5,16,21,24] The formation of this hydrogen-bonding network, reinforced by hydrophobic packing, results in very poor solubility of the material in water as has been observed in many amyloid-like materials. To mitigate this, flanking block **A** containing a variable number of charged amino acids (in this case lysine, K) was added to both termini.

MDPs were synthesized with a variable number of QL repeats and K residues including peptides $K_2(QL)_mK_2$ where $m = 2-6$ and peptides $K_n(QL)_6K_n$ where $n = 0-4$ for a total of nine peptides studied. Experimental methods including synthesis, purification, and characterization of the peptides are described in the Supporting Information.

$K_2(QL)_mK_2$ Series. The secondary structure and the corresponding nanostructural morphology were examined by circular dichroism (CD) spectroscopy and vitreous ice cryo-transmission electron microscopy (cryo-TEM) at pH 7.4 at a concentration of 1% by weight (5 mM for $K_2(QL)_6K_2$) and in the presence of 10 mM Tris buffer. At pH 7.4, all the MDPs remain soluble in water owing to the charge repulsion existing on the termini (with the exception of $K(QL)_6K$ and $(QL)_6$ which are insoluble at all pH values, see Supporting Information). CD spectra indicate three secondary structures and two nanostructures adopted by the peptides depending on the balance between the block driving self-assembly (QL) and the block mitigating assembly. $K_2(QL)_2K_2$, $K_2(QL)_3K_2$ and $K_2(QL)_4K_2$ show only random coil conformation and cryo-TEM shows only amorphous aggregates (Figure 2a−f). This is expected since in order for long range assembly to take place the packing of only two, three, or four leucine residues must compensate for the charge repulsion of four lysines. When a peptide contains five QL repeats ($K_2(QL)_5K_2$), it shows a markedly different CD spectrum, no longer representative of a random coil, but instead a weak β-sheet conformation (Figure 2g). At the same time cryo-TEM reveals a mixture of small amorphous aggregates or vesicles with a significant population of short nanofibers with a diameter of 5 $\pm$ 1 nm (Figure 2h). The presence of five leucines is just able to balance the electrostatic repulsion of lysine, but the population is not uniform containing significant fractions of both amorphous and fibrous morphologies. The appearance of nanofibers is believed to be due to peptide's secondary structural transition into organized β-sheet aggregates. Adding one additional QL repeat, $K_2(QL)_6K_2$ shows a very strong β-sheet conformation by CD (Figure 2i) and a population of nanofibers with uniform diameter (6 $\pm$ 1 nm), controlled length (120 $\pm$ 30 nm), and no amorphous aggregates by cryo-TEM (Figure 2j, seven cryo-TEM images under these conditions are available in the Supporting Information, Figure SI-1a−g). The hydrophobic packing of six leucines is able to compensate for the charge repulsion of four lysine residues and large nanostructured fibers are able to form. However, the balance between assembly and disassembly is close enough that fibers terminate after a finite length, most likely from the additive long-range effects of electrostatic repulsion which can be eliminated on the basis of pH or screening by salt (see below).

The model proposed in Figure 1 predicts a width of 5.4 nm for each individual nanofiber formed by $K_2(QL)_6K_2$. This assumes polyproline type II conformation adopted by charged lysine residues and an extended β-sheet conformation for QL repeating units. This is in good agreement with our experimental results which show a fiber diameter of 6 $\pm$ 1 nm. Molecular modeling suggests a fiber depth of 2 nm which is not observed by cryo-TEM, perhaps due to the flexibility of the peptide

(15) Janek, K.; Behlke, J.; Zipper, J.; Fabian, H.; Georgalis, Y.; Beyermann, M.; Bienert, M.; Krause, E. *Biochemistry* **1999**, *38*, 8246−8252.
(16) Yokoi, H.; Kinoshita, T.; Zhang, S. G. *Proc. Natl. Acad. Sci.* **2005**, *102*, 8414−8419.
(17) Schneider, J. P.; Pochan, D. J.; Ozbas, B.; Rajagopal, K.; Pakstis, L.; Kretsinger, J. *J. Am. Chem. Soc.* **2002**, *124*, 15030−15037.
(18) Pochan, D. J.; Schneider, J. P.; Kretsinger, J.; Ozbas, B.; Rajagopal, K.; Haines, L. *J. Am. Chem. Soc.* **2003**, *125*, 11802−11803.
(19) Ozbas, B.; Kretsinger, J.; Rajagopal, K.; Schneider, J. P.; Pochan, D. J. *Macromol.* **2004**, *37*, 7331−7337.
(20) Veerman, C.; Rajagopal, K.; Palla, C. S.; Pochan, D. J.; Schneider, J. P.; Furst, E. M. *Macromolecules* **2006**, *39*, 6608−6614.
(21) Dong, H.; Hartgerink, J. D. *Biomacromolecules* **2006**, *7*, 691−695.
(22) Dong, H.; Hartgerink, J. D. *Biomacromolecules* **2007**, *8*, 617 - 623.
(23) Krause, E.; Beyermann, M.; Fabian, H.; Dathe, M.; Rothemund, S.; Bienert, M. *Int. J. Pept. Protein Res.* **1996**, *48*, 559−568.
(24) Kammerer, R. A.; Kostrewa, D.; Zurdo, J.; Detken, A.; García-Echeverría, C.; Green, J. D.; Müller, S. A.; Meier, B. H.; Winkler, F. K.; Dobson, C. M.; Steinmetz, M. O. *Proc. Natl. Acad. Sci.* **2004**, *101*, 4435−4440.

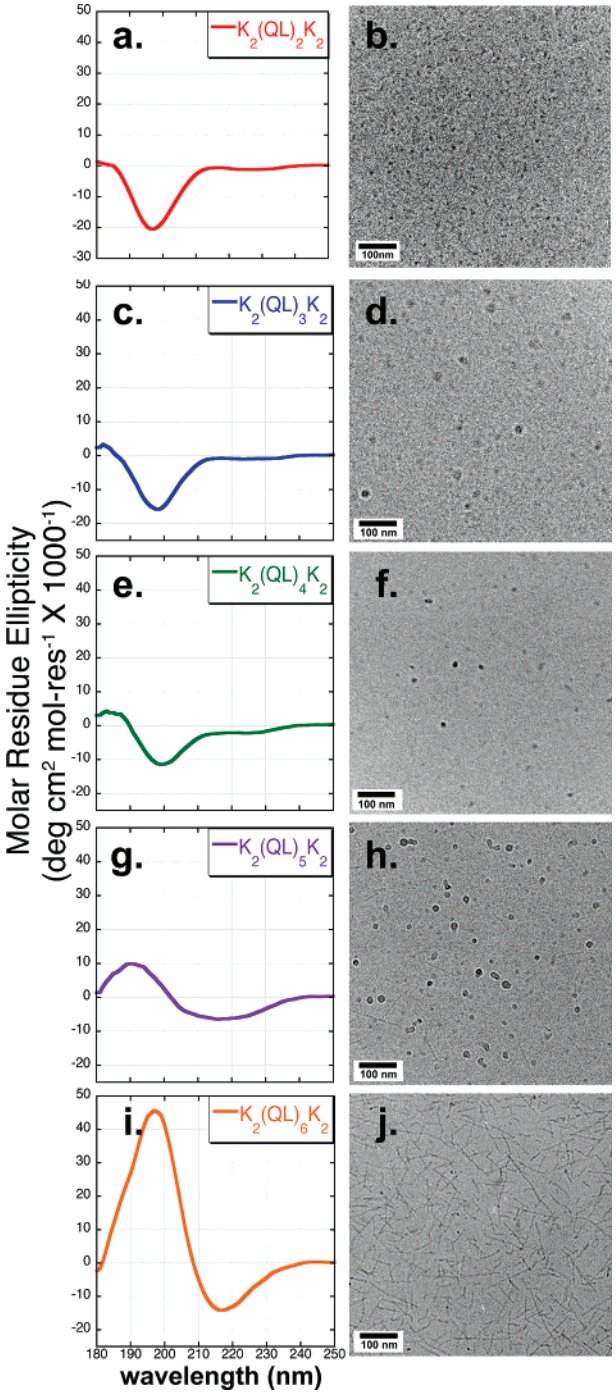

Figure 2. CD spectra and corresponding cryo-images of K2 series of peptides at neutral pH. (a, b) CD and TEM of $K_2(QL)_2K_2$, (c, d) CD and TEM of $K_2(QL)_3K_2$, (e, f) CD and TEM of $K_2(QL)_4K_2$, (g, h) CD and TEM of $K_2(QL)_5K_2$, (i, j) CD and TEM of $K_2(QL)_6K_2$.

chains. However, when peptide fibers are dried onto freshly cleaved mica and examined by AFM, a uniform height of 2 nm is measured in good agreement with our model (see Supporting Information Figures SI-11−13).

Oriented FT-IR studies can be used to determine the orientation of hydrogen bonding with respect to the fiber long axis.[6] $K_2(QL)_6K_2$ was spin coated onto both a CaF_2 window and a gold mirror. FT-IR was performed normal to the CaF_2 surface (and thus normal to the fiber long axis) and at an 80° grazing angle from the gold mirror (thus 10° off parallel with the fiber axis). In the grazing angle it can be observed that the

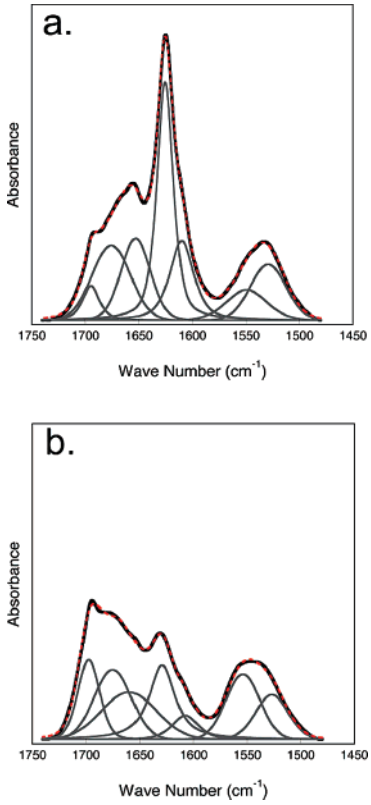

Figure 3. FT-IR of the amide I and amide II region of $K_2(QL)_6K_2$: (a) sample examined after spin coating onto a CaF_2 window with the IR beam normal to the window (and thus the fiber long axis) surface; (b) sample spin coated onto gold mirror and examined by grazing angle (80°) IR. Spectra were baseline corrected and deconvoluted, shown in gray.

amide I band at 1625 cm^{-1} (indicating β-sheet) is greatly attenuated (Figure 3b) with respect to the normal FT-IR (Figure 3a). This indicates the orientation of the hydrogen bonding is, as expected, parallel to the fiber long axis. Furthermore FT-IR shows a strong antiparallel component, particularly in the grazing angle mode where this band is enhanced, at 1692 cm^{-1}. This confirms our model of assembly demonstrating that the hydrogen bonding is an antiparallel β-sheet with the axis of hydrogen-bonding parallel to the nanofiber and the peptide backbone oriented perpendicular to the fiber axis.

$K_n(QL)_6K_n$ Series. The next series of peptides examined the effect of changing the number of lysines in the **A** block while holding the number of QL repeats constant at six. $(QL)_6$ and $K(QL)_6K$ were found to be completely insoluble at all pH values examined (2−12). Therefore even when all lysines are protonated, the repulsion between them is not sufficient to stop aggregation between the six leucine residues. In neat TFA $(QL)_6$ is soluble, presumably when backbone charging begins to take place. However, addition of even moderate quantities of water resulted in their precipitation. TEM images of these precipitates showed dense clusters of entangled fibers (Figure SI-2). FT-IR revealed strong β-sheet secondary structure (Figure SI-3). A second lysine in the **A** block resulted in individually dispersed nanofibers described above which remain soluble. Adding a third lysine is sufficient to largely disrupt the self-assembled fibrous structure. Cryo-TEM of $K_3(QL)_6K_3$ (Figure SI-4b) shows mostly small amorphous aggregates with a small population of nanofibers with lengths somewhat shorter than the lengths of fibers from $K_2(QL)_6K_2$. Adding a fourth lysine on both termini totally

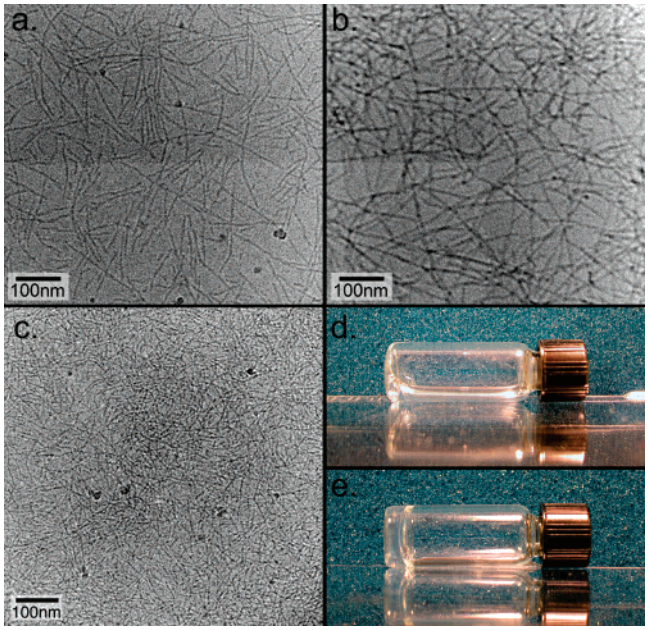

Figure 4. (a) $K_2(QL)_6K_2$ at 1 wt % in the presence of 150 mM NaCl and 10 mM Tris. (b) $K_2(QL)_6K_2$ at 1 wt % in the presence of 1 M NaCl and 10 mM Tris. (c) Cryo-TEM image of peptide $K_2(QL)_6K_2$ at 1 wt % concentration and at pH 12. The formation of dense network of long fibers can be seen. (d) $K_2(QL)_6K_2$ at 1 wt % in 10 mM Tris at pH 7. (e) $K_2(QL)_6K_2$ at 1 wt % in 150 mM NaCl and 10 mM PO_4.

eliminates the presence of fibers (Figure SI-4c). Corresponding CD spectra indicate the simultaneous secondary structural change from β-sheet to weak α-helix as the number of lysines is increased (Figure SI-5).

Electrostatic Screening and pH. If charge repulsion is the primary force preventing aggregation of these fibers, increasing ion concentration or pH should increase the fiber length. To test this, samples of $K_2(QL)_6K_2$ were prepared in 10 mM Tris pH 7.4 with 150 mM NaCl. Vitreous ice cryo-TEM reveals fibers with length increased to 150 $\pm$ 45 nm (Figure 4a), but these samples remain soluble and do not gel. Increasing the NaCl concentration to 1 M resulted in a highly viscous solution and dramatically increased fiber length ("infinite" length) as observed by TEM (Figure 4b). Exceeding the pK_a of lysine at a pH of 12 effectively eliminates all charge on the peptide. The peptide in this solution rapidly aggregates as a white suspension which eventually precipitates. CD shows that at pH 12 all the peptides, except $K_2(QL)_2K_2$, fold into β sheets characterized by a single minimum at approximately 220 nm (Figure SI-6). Sonicated dispersions of the high pH precipitate examined by cryo-TEM (Figure 4c) reveal a dense matrix of infinite length fibers. Nanofibers formed by MDPs at high pH indicate that without designed charge control, peptides form long, insoluble entangled nanofibers. Previously, amyloid-like nanofibers have been reported to have sizes mostly on the order of several micrometers, and those fibers tend to form insoluble aggregates.[5,16,21,24] Our observations demonstrate that we can balance forces of assembly against forces of disassembly to control fiber size and aggregation.

The presence of multivalent anions such as phosphate result in the formation of clear, self-supporting gels. In particular, $K_2(QL)_6K_2$ in phosphate-buffered saline (PBS) containing 150 mM NaCl and 10 mM phosphate at a pH of 7 forms gels which may be suitable for cell entrapment and growth (Figure 4d,e).

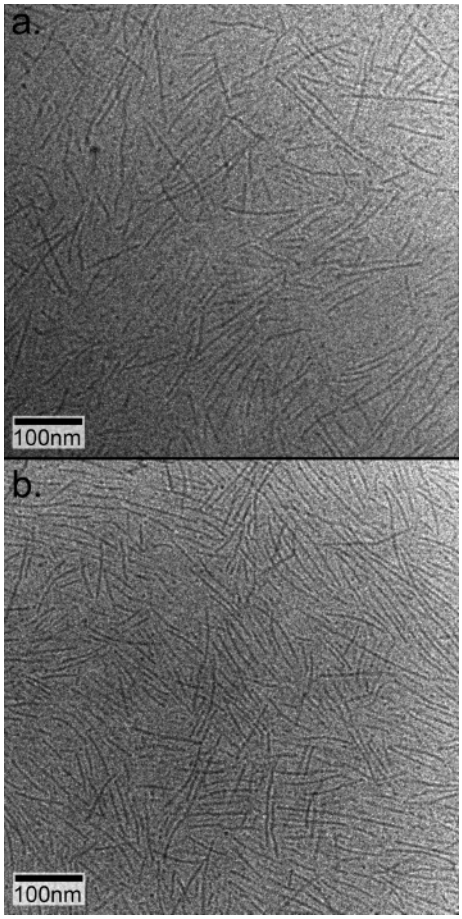

Figure 5. Aged samples of $K_2(QL)_6K_2$: (a) 0.5% by weight (b) 1% by weight. The image in panel a was prepared from a 1% by weight solution that was diluted 1:1 with 10 mM Tris buffer immediately before plunging into an ethane slush for vitrification to easier visualization of fiber ends which are more difficult to see at higher concentration.

Notably, exclusion of phosphate from the solution eliminates gel formation. The phosphate likely acts as a physical cross-linking agent with the positively charged lysine residues.

Aging. Many examples of peptide fibrillation undergo a ripening phenomenon in which fiber length and/or width increase over time.[7] This process indicates that the initially formed fibrous structure is not the thermodynamic minimum and the system is still moving toward equilibrium composed of larger or bundled fibers. This process was examined in our system. The sample in Figure 1i,j was examined within several hours of preparation using dynamic light scattering (DLS), CD, FT-IR, and vitreous ice cryo-TEM. Figure 5 shows fibers of $K_2(QL)_6K_2$ which have aged for three weeks. The maximum fiber lengths have not changed substantially from those observed in Figure 1j. The average lengths, however, have increased somewhat, owing to the disappearance of shorter fibers. Analysis by DLS supports this finding (Figure SI-7). FT-IR and CD have not significantly changed over time. Additionally the sample did not precipitate or form a gel.

The assembly of MDPs into organized fibers can be attributed primarily to three types of interactions. First, hydrophobic packing of leucine side chains is the primary thermodynamic driving force for assembly in water, but does not provide control over shape or structure. Second, backbone β-sheet hydrogen bonding also contributes to the stability of the assembly but is more important in directing the anisotropy of the structure.

Third, these forces are opposed by electrostatic repulsion between lysine side chains. As one changes the ratio between the number of hydrophobic residues and charged residues one may shift the equilibrium toward either self-assembly or disassembly. Therefore, fabrication of nanofibers with controlled-length becomes possible when the driving force of the self-assembly of $(QL)_m$ subunits and opposing charge repulsion forces are balanced. On the basis of our results, when m/n is ≥ 3, nanofibers with controlled dimension are produced.

Conclusions

We have designed a series of multidomain peptides which adopt defined secondary structure at neutral pH based on their primary structural composition. The ratio m/n determines the peptides' secondary structures, which then dictates the peptides' supramolecular structure. It is important to note that at neutral pH, $K_2(QL)_6K_2$ self-assembles into β-sheets which are soluble in water. This observation is rare among peptides which form β-sheet assemblies which tend to generate insoluble materials. Our peptides may find use in understanding and treating various diseases caused by protein aggregation in addition to being used as nanostructured scaffolds for bioengineering applications.

Acknowledgment. We would like to thank S. B. Kadali and M. Wong for assistance with DLS. J.D.H. gratefully acknowledges his Searle Scholar Award. This work was funded by The Welch Foundation research Grant C1557, NSF CAREER Award DMR-0645474, and The Alliance for Nanohealth.

Supporting Information Available: Synthetic methods, CD, grazing angle, and transmission FT-IR, AFM, cryo-TEM images, and DLS. This material is available free of charge via the Internet at http://pubs.acs.org.

JA072536R